An Enhanced Hybrid Springback Compensation Approach: Springback Path – Displacement Adjustment Method For Complex Shaped Products of Sheet Metal Forming

Zhihui Gong
Hunan University
Mandeep Singh
University of Technology Sydney
Bohao Fang
Hunan University
Dongbin Wei (dongbin.wei@uts.edu.au)
University of Technology Sydney https://orcid.org/0000-0002-4247-8905

Research Article

Keywords: Springback, Compensation, Sheet metal forming, FEM

Posted Date: October 18th, 2021

DOI: https://doi.org/10.21203/rs.3.rs-980113/v1

An Enhanced Hybrid Springback Compensation Approach: Springback Path – Displacement Adjustment Method for Complex Shaped Products of Sheet Metal Forming

Zhihui Gong[1], Mandeep Singh[2], Bohao Fang[1], Dongbin Wei[2*]

[1]State Key Laboratory of Advanced Design and Manufacture for Vehicle Body, Hunan University, Changsha, 410082, China.

[2]School of Mechanical and Mechatronic Engineering, University of Technology Sydney, 2007, NSW, Australia.

Abstract

Springback compensation is critical in sheet metal forming. Advanced techniques have been adopted in the design stage of various sheet metal forming processes, e.g. stamping, some of which are for complex shaped products. However, the currently available numerical approaches are not always sufficiently accurate and reliable. To improve the accuracy of springback compensation, an enhanced hybrid springback compensation method named Springback Path – Displacement Adjustment (SP-DA) method has been developed in this study based on the well-known conventional displacement adjustment (DA) method. Its effectiveness is demonstrated using FEM analysis of low, medium and high strength steels adopted in automobile industry, in which a symmetrical model owning geometry complexity similar to an auto body panel was established. The results show this new enhanced SP-DA method is able to significantly improve the accuracy of springback compensation comparing to conventional displacement adjustment technique.

Key words: Springback; Compensation; Sheet metal forming; FEM

1. Introduction

Cracking, wrinkling and springback are the most common defects in sheet metal forming, e.g. stamping while springback is the hardest to handle [1-3]. Springback is a process in which the internal stress in a part is released after removing the constraint of the die or trimming addendum surface [4-5]. It may lead to undesirable geometries and rejected products [6-7]. Currently the issue of springback may be resolved in the stage of pre-production or post-production. The pre-production solution is to alter tool geometry manually based on the difference between the actual and target dimensions of the fabricated parts [8]. Theoretically this method may completely eliminate springback, but it could incur high cost and much time to achieve an accurate profile for compensation. The post-production solution is to adjust process parameters, e.g. increasing blank holder force or restrain force of drawbead so both the inner and outer sides of a sheet metal forming product are subjected to tensile stress [9]. This may partly reduce springback while increase the risk of cracking. Pre-production solution is preferred when it is possible. Springback needs to be determined using numerical methods

* Corresponding Author: Tel: +61-295147528; Email: Dongbin.Wei@uts.edu.au

before a compensation may be conducted at the stages of design and construction of a stamping die [10], as illustrated in Fig. 1. Springback compensation mesh is acquired through an iterative algorithm integrating the numerical simulation and analysis of springback at the stage of design [11], based on which the die may be manufactured. The deviation between an actual stamping product and its design needs to be checked. If further springback compensation is necessary, the actual stamping product may be scanned for creating a modified mesh to further modify the die [12-13]. This study focuses on springback compensation in the stage of design.

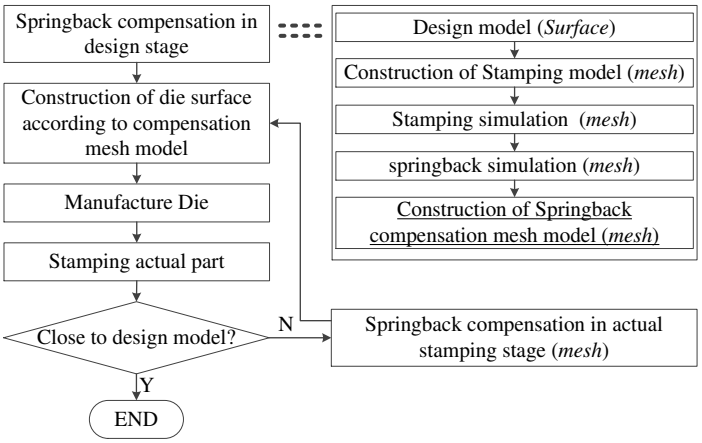

Figure 1 The process of springback compensation in stamping

Geometric features need to be considered when determining the exact position of each node in the springback compensation mesh. For example, as shown in Fig. 2, node i locates in a flat section in the design model. Its corresponding node in the springback compensation mesh may be located at i_1'' or i_2'', which has little influence on the construction of the new surface. On the other hand, for node j locating at the edge of an arc, the position of its corresponding node j'' in the springback compensation mesh needs to be determined cautiously for ensuring the geometrical feature is transferred to the new surface properly.

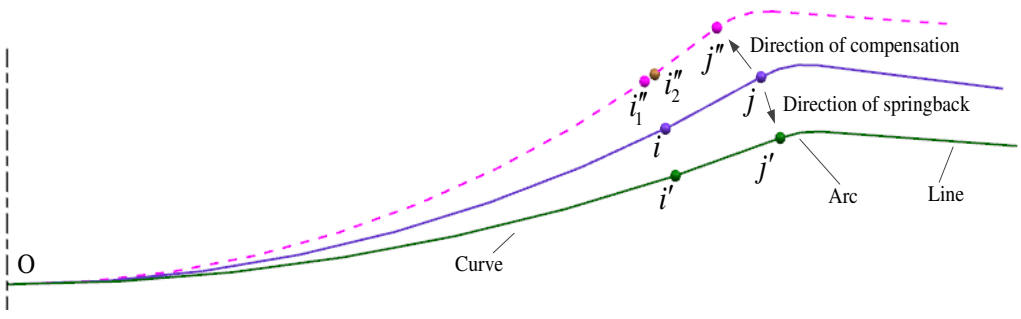

Figure 2 Consideration of geometric features when determining the position of a node in springback compensation mesh

Two methods have been developed to construct the surface for springback compensation. One is force descriptor method (FDM) proposed by Karafillis and Boyce [14], which is a stress reverse iteration compensation method. Reverse springback can be obtained by artificially reversing the stress in inner and outer layers of a sheet. It may be hard to achieve convergence

in the iterative calculation in the case of large springback and asymmetric parts. In order to improve the condition of convergence, Wu [15-16] introduced a factor determined by the deviation of the key dimension of the part to multiply the stress. Anagnostou [17] proposed a modified FDM by introducing a compensation coefficient based on the distance between the positions of a node before and after springback. However, these cannot completely resolve the issue of convergence.

The other method is geometric compensation based on the displacement of a node, which has been widely adopted. The distance between the positions of a node before and after springback along the moving direction of the tool is set as the value of springback compensation. Using displacement adjustment (DA) method [18], a node is moved to the spring compensation mesh along the direction opposite to the moving direction of the tool, which has relatively fast convergence. DA method is effective for most areas in a part except for side wall because the compensation direction on side wall is perpendicular to the moving direction of the tool. Weiher [19] proposed a modified DA method, in which the distance between the position of a node before and after springback is taken as springback value and compensation is carried out along the direction simply opposite to the direction of springback. The method has good convergence, however, it may incur large errors when the springback is large or the product has a complex shape. Yang [20] proposed another modified DA method by introducing an angle compensation coefficient. It has high accuracy and efficiency for simple shaped parts but it is not an easy task to determine the angle coefficient everywhere in a complex shaped part.

Considering the significant influence of the complexity of a sheet metal forming product on spring compensation, there is still a large room for further research. The aim of this study is to develop an enhanced hybrid springback compensation approach, i.e. Springback Path - Displacement Adjustment (SP-DA) method for acquiring accurate springback compensation mesh taking into account all geometric features. The springback compensation mesh is used to construct the surface of tools iteratively till the target may be achieved in numerical simulation. The results obtained using this new enhanced approach are compared with those obtained using Weiher's method.

2. Methodology

It is assumed that the moving path of a node during springback and compensation are always similar. Springback compensation does not change die design parameters, binder surface, addendum surface, complexity of the surface and geometrical features. A symmetrical model owning a geometrical complexity that is similar to that of auto body panel was established and finite element method (FEM) simulation was carried to acquire springback at every node by employing commercial package LS-DYNA. The thickness of the blank is 1mm. Three steels ST14F, BH300 and DP500 were adopted, which represent low, medium and high strength steel respectively adopted in automobile industry for observing the effect of the strength on springback. The nominated chemical compositions and mechanical properties of these steels are shown in Table 1 and Table 2 respectively.

Table 1 Chemical compositions (wt%)

Materials	C	Mn	P	S	Al	Fe
ST14F	≤0.08	≤0.4	≤0.03	≤0.03	≥0.02	Balanced

BH300	≤0.1	≤1.5	≤0.12	≤0.025	≥0.01	Balanced
DP500	≤0.15	≤2.5	≤0.04	≤0.015	≥0.01	Balanced

Table 2 Mechanical properties

Materials	ρ (kg/m^3)	E (GPa)	μ	K	n	Plastic anisotropy		
						R_0	R_{45}	R_{90}
ST14F	7.85	207	0.28	537.1	0.219	1.84	1.22	2.6
BH300				726	0.18	1.09	0.80	1.4
DP500				802	0.15	1.00	0.87	1.05

The stress-strain relationship is described by

$$\sigma = K\varepsilon^n \qquad (1)$$

where σ is true stress, ε is true strain, K is hardening coefficient, n is hardening exponent.

2.1 Algorithm

As shown in Fig. 3(a), N_o and N_{sp} represent two corresponding nodes on the meshes of a stamping part before and after springback respectively. N_i (i = 1, 2, ..., n) are the points on the springback path between N_o and N_{sp}. The curve of springback path C^N_{o-sp} can be constructed by interpolation as shown in Fig. 3(b).

(a) (b)

Figure 3 Construction of springback path

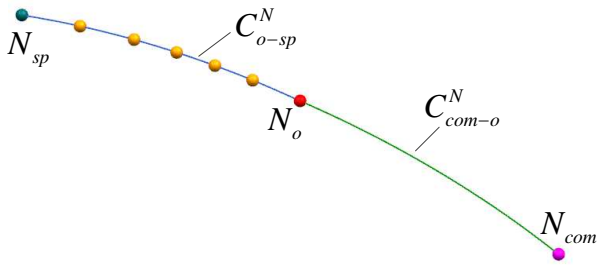

Figure 4 Construction of springback compensation path

As shown in Fig. 4, N_{com} is the node on the mesh of springback compensation and C^N_{com-o} is the curve of springback compensation path. The curves C^N_{com-o} and C^N_{o-sp} are similar and continuous, i.e. the tangent direction at point N_o must be unique. Below is the method of

acquiring N_{com}.

- To calculate the two unit tangent vectors $V_{sp}^N(V_{sp-x}^N, V_{sp-y}^N, V_{sp-z}^N)$ and $V_o^N(V_{o-x}^N, V_{o-y}^N, V_{o-z}^N)$ at the end points $N_{sp}(N_{sp}^x, N_{sp}^y, N_{sp}^z)$ and $N_o(N_o^x, N_o^y, N_o^z)$ on curve C_{o-sp}^N, as shown in Fig. 5(a).
- To translate curve C_{o-sp}^N and let N_{sp} coincide with N_o as shown in Fig. 5(b). The angle θ between V_{sp}^N and V_o^N can be calculated by dot product of V_{sp}^N and V_o^N. V_r^N is the unit vector vertical to the plane formed by V_{sp}^N and V_o^N, which can be calculated by the cross product of V_{sp}^N and V_o^N. $N_o'(N_{o-x}', N_{o-y}', N_{o-z}')$ representing the new position of N_o after the translation, which can be determined using equation (2).

$$\begin{cases} N_{o-x}' = 2 \times N_o^x - N_{sp}^x \\ N_{o-y}' = 2 \times N_o^y - N_{sp}^y \\ N_{o-z}' = 2 \times N_o^z - N_{sp}^z \end{cases} \qquad (2)$$

- As shown in Fig. 5(c), to rotate curve C_{o-sp}^N and unit vector V_{sp}^N about an axis going through unit vector V_r^N at an angle θ so V_{sp}^N aligns with V_o^N then the position of node N_{com} may be determined.

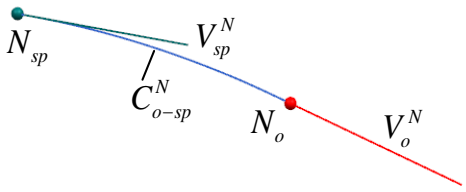

(a)

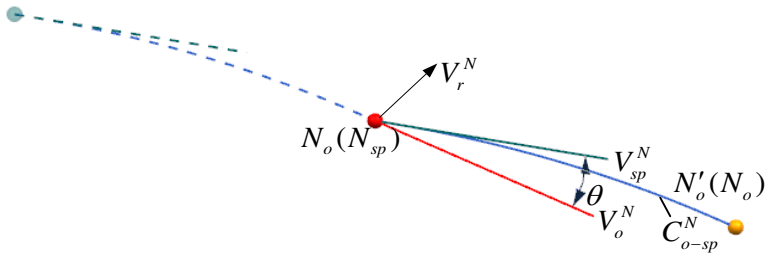

(b)

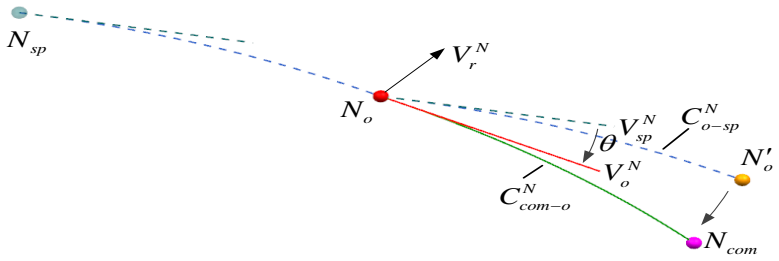

(c)

Figure 5 Method of determining the position of a node on the mesh of springback compensation

2.2 FEM simulation of forming process

A model of stamping part owning sufficient geometry complexity was carefully designed as shown in Fig. 6 (a). Only a quarter needs to be considered in the FEM simulation considering the symmetry, as shown in Fig. 6 (b). The dimensions are shown in Fig. 7. The paths of four locations A, B, C and D sitting on four featured curves AO, AB, BC and CD are focused. The lengths of these curves are 322.80, 282.29, 130.72 and 188.89 mm respectively.

(a) (b)

Figure 6 (a) A model of stamping part owning sufficient geometry complexity; (b) a quarter of the model for FEM simulation

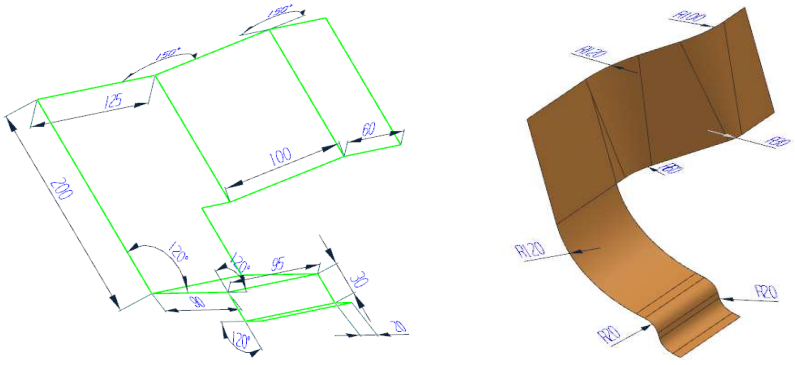

Figure 7 Dimensions of the simulation model (unit: mm)

The profiles of the blank before and after stamping are shown in Fig. 8(a). The profile of the die in the simulation is constructed according to that of the part as shown in Fig. 8(b). Explicit FEM was carried out using symmetrical boundary condition as shown in Fig. 8(c). The

die moves down while the punch at bottom is fixed. A fixed pad is set to be 3 mm away from the punch for restraining the overarching of the middle part of the blank during stamping. The die, punch and pad are defined as rigid body. Both the tools and blank are meshed and the mesh size is 3 mm. The blank adopts BT element and there are 5 Gauss integral points along its thickness direction. There are 42558 shell elements, including 41979 quadrangle elements and 579 triangular elements. The speed of the die is 2 m/s. The gap between the punch and die is 1 mm at the end of the simulation.

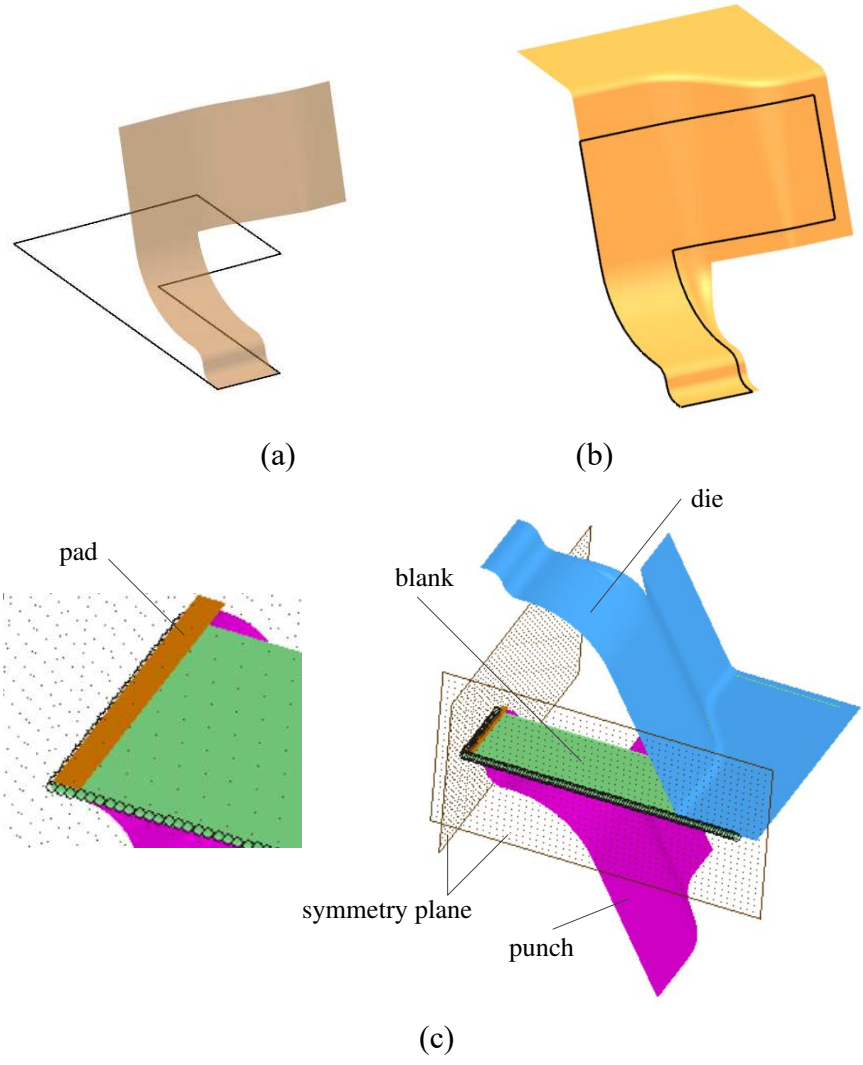

Figure 8 FEM simulation model

2.3 FEM analysis on springback

Implicit FEM was adopted in the analysis on springback after the forming tools are removed. The forces at all nodes at the end of the simulation of stamping are applied in the beginning of this analysis as boundary condition. The forces were released in ten steps and 10% of total force was released in each step to acquire ten positions of each node during springback for constructing the moving path of the node. Full integration element is adopted in the blank. In order to define springback, 66 nodes on bottom plane were selected as reference, i.e. they were constrained in three direction of x, y and z, as shown in Fig. 9.

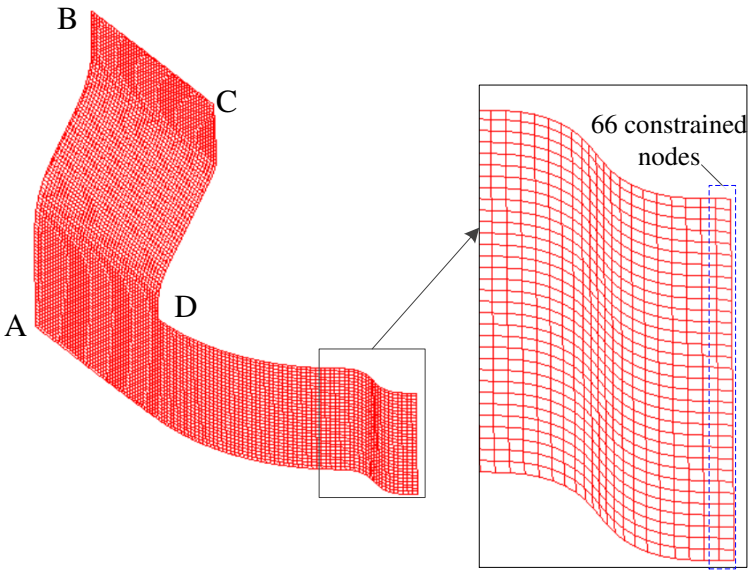

Figure 9 66 nodes on bottom plane selected as reference in the analysis of springback

3. Results and discussion

3.1 Comparison of springback using SP-DA and DA methods

FEM analysis results of springback after 100% unloading are shown in Fig. 10. The displacements at locations A, B, C and D after springback are listed in Table 3.

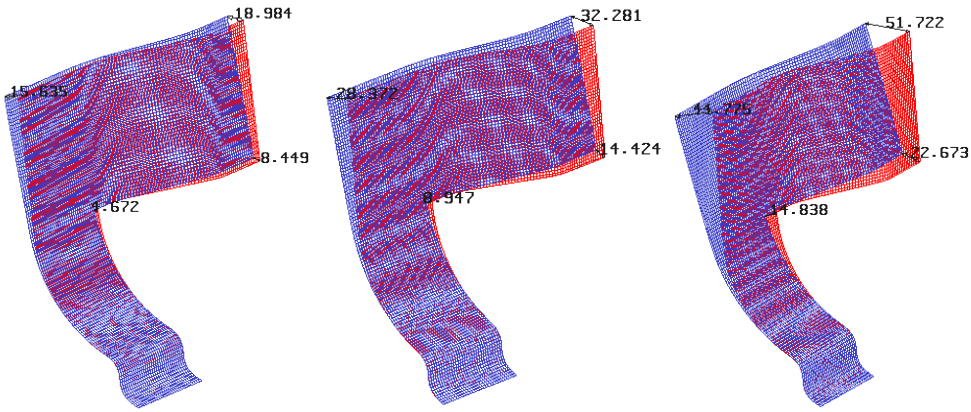

(a) ST14F (b) BH300 (c) DP500

Figure 10 FEM analysis results of springback after 100% unloading

Table 3 Displacements at locations A, B, C and D after springback (mm)

	ST14	BH300	DP500
A	15.635	28.372	44.775
B	18.984	32.281	51.772
C	8.449	14.424	22.673
D	4.672	8.947	14.838

Table 4 shows the displacement at location B that is farthest from the reference points after each step of unloading for further investigation. The values after steps 1 to 9 are much smaller than that in the tenth step, i.e. the first nine position points are very much close. This is because the forces at all nodes at the end of stamping are much higher than the internal stress that causes springback due to the existence of blank hold force etc.

Table 4 Displacement location B after each unloading step (mm)

Material	1	2	3	4	5	6	7	8	9	10
ST14F	0.47	0.471	0.473	0.477	0.484	0.497	0.524	0.581	0.755	18.984
BH300	0.987	0.998	1.012	1.03	1.054	1.086	1.134	1.221	1.456	32.281
DP500	1.428	1.462	1.503	1.552	1.612	1.69	1.797	1.964	2.327	51.722

In order to acquire evenly distributed position points for generating the springback path by interpolation, a specific elastic modulus was assigned in each step from step 1 to step 8. This method does not change the springback path. Table 5 shows the specific elastic modulus assigned and the displacements at locations A, B, C and D in steps 1 – 8 in the case of steel ST14F. The results at location B are illustrated in Fig. 11.

Table 5 Assigned elastic modulus and displacement after each unloading step at locations A, B, C and D in steel ST14F

	1	2	3	4	5	6	7	8
E(GPa)	1177	677	497	377	317	277	237	207
A (mm)	2.756	4.792	6.526	8.600	10.224	11.697	13.665	15.635
B (mm)	3.329	5.788	7.887	10.404	12.379	14.173	16.571	18.984
C (mm)	1.479	2.571	3.503	4.623	5.502	6.302	7.37	8.449
D (mm)	0.597	1.190	1.632	2.118	2.737	3.253	3.857	4.672

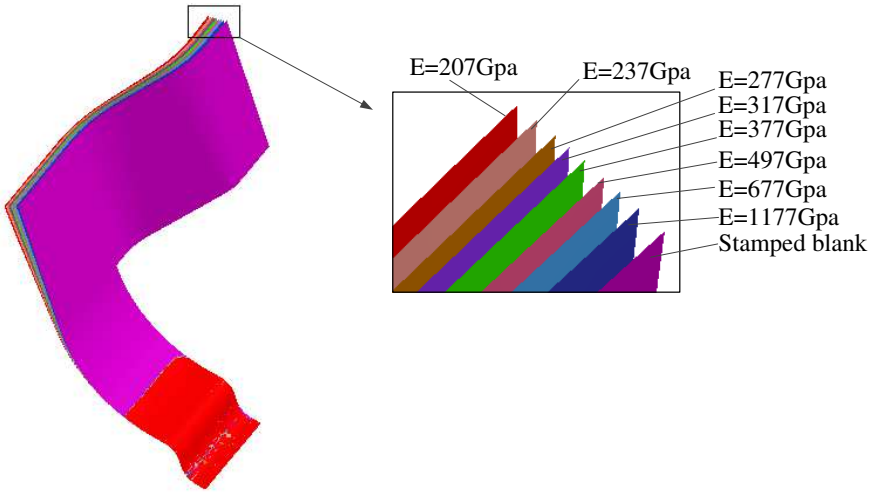

Figure 11 Specific elastic modulus assigned and the analysis results of springback at location B in ST14F

The coordinate of each point needs to be obtained. For a group of position points

$P_i(x_i, y_i, z_i)$, i = 0, 1,…, n, a cubic parameter accumulated chord length spline interpolation method described in Equation (3) is applied to determine the accumulated chord length of each point.

$$\begin{cases} s_0 = 0 \\ s_1 = l_1 = \sqrt{(x_1 - x_0)^2 + (y_1 - y_0)^2 + (z_1 - z_0)^2} \\ s_2 = l_1 + l_2 = s_1 + \sqrt{(x_2 - x_1)^2 + (y_2 - y_1)^2 + (z_2 - z_1)^2} \\ s_k = \sum_{j=1}^{k} l_k = \sum_{j=1}^{k} |P_j - P_{j-1}| = \sum_{j=1}^{k} \sqrt{(x_j - x_{j-1})^2 + (y_j - y_{j-1})^2 + (z_j - z_{j-1})^2} \\ k = 1,2,....., n \end{cases} \quad (3)$$

where s_k is accumulated chord length of position point, l_k is chord length between two adjacent points, as shown in Fig.12.

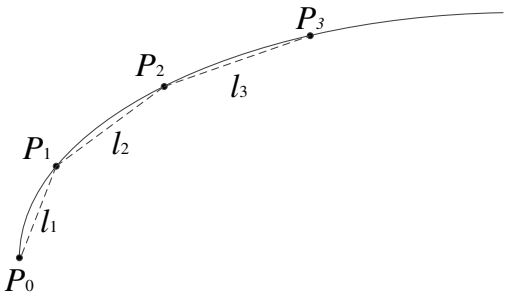

Figure 12 A spline constructed by accumulated chord length method

The relationship between s and x, y and z at each point is shown in Table 6, which can be used for obtaining $x = x(s), y = y(s), z = z(s)$.

Table 6 Relationship between s and x, y and z

S	s_0 s_1 s_2 … s_n
X	x_0 x_1 x_2 … x_n
Y	y_0 y_1 y_2 … y_n
Z	z_0 z_1 z_2 … z_n

Equation (4) is based on the condition of continuity at each point.

$$x_j''(s_j^-) = x_{j+1}''(s_j^+) \quad j=1, 2, \ldots, n\text{-}1 \quad (4)$$

Equation (5) may be achieved.

$$m_{j-1}^x \frac{h_{j+1}}{h_j + h_{j+1}} + 2m_j^x + m_{j+1}^x \frac{h_j}{h_j + h_{j+1}} = 3\left[\frac{h_{j+1}}{h_j + h_{j+1}} \frac{x_j - x_{j-1}}{h_j} + \frac{h_j}{h_j + h_{j+1}} \frac{x_{j+1} - x_j}{h_{j+1}}\right] \quad (5)$$

where j=1, 2,…, n-1, $h_j = s_j - s_{j-1}$, and m_j^x is the component on x axis of the first derivative.

The second derivative of two endpoints are specified as zero so equation (6) may be obtained.

$$\begin{cases} 2m_0^x + m_1^x = \dfrac{3(x_1 - x_0)}{s_1 - s_0} \\ m_{n-1}^x + 2m_n^x = \dfrac{3(x_n - x_{n-1})}{h_n - h_{n-1}} \end{cases} \tag{6}$$

m_j (j=0, 1, …, n) can be obtained from equation (5) and equation (6).

$x(s)$ can be worked out using equation (7).

$$x(s) = m_{j-1}\frac{(s_j - s)^2(s - s_{j-1})}{h_j^2} - m_j\frac{(s - s_{j-1})^2(s_{j-s})}{h_j^2} + x_{j-1}\frac{(s_j - s)^2[2(s - s_{j-1}) + h_j]}{h_j^3} + x_j\frac{(s - s_{j-1})^2[2(s_j - s) + h_j]}{h_j^3} \tag{7}$$

where $h_j = s_j - s_{j-1}, s_{j-1} \le s \le s_j$

The similar procedure was used for $y(s)$ and $z(s)$. Then the curve of springback path may be created.

Adopting the method described in section 2.1, the tangent vectors of two endpoints on the meshes before and after spingback can be calculated, followed by the determination the spring compensation path, then the construction of spring compensation mesh.

The results obtained using SP-DA method are compared to those obtained using DA method, as shown in Figs. 13 – 15 for ST14F, BH300 and DP500 respectively.

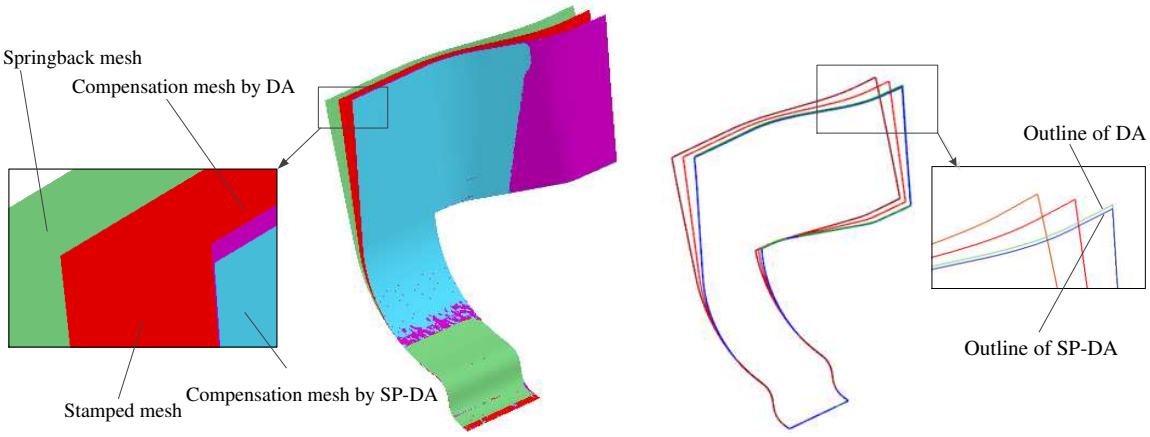

(a) Meshes (b) Outlines

Figure 13 Comparison of the meshes and outlines of springback and springback compensation obtained using SP-DA method and DA method in ST14F

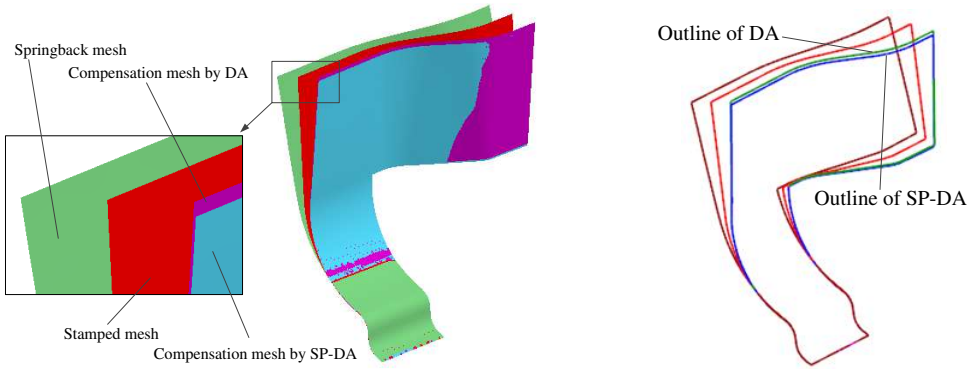

(a) Meshes (b) Outlines

Figure 14 Comparison of the meshes and outlines of springback and springback compensation obtained using SP-DA method and DA method in BH300

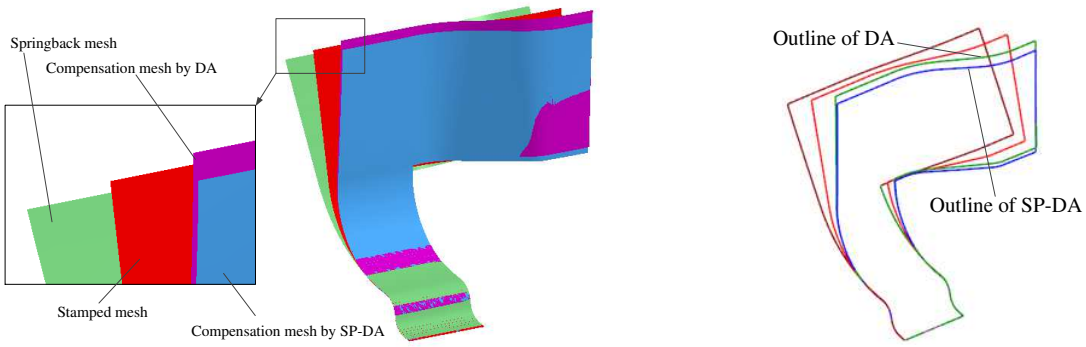

(a) Meshes (b) Outlines

Figure 15 Comparison of the meshes and outlines of springback and springback compensation obtained using SP-DA method and DA method in DP500

The lengths of the four curves are listed in Table 7. V_d represents the lengths in CAD model. V_f and V_s represent the lengths before and after springback respectively. V_{DA} represents the length after springback using DA method and V_{SP-DA} represents the length after springback using SP-DA method.

Table 7 The lengths of the curves obtained using SP-DA and DA methods (mm)

Arc	V_d	Material	V_f	V_s	V_{DA}	Dev_{DA}	V_{sp-DA}	Dev_{sp-DA}
S_{AO}	322.8	ST14F	322.584	322.668	323.740	1.240	322.583	0.083
		BH300	322.557	322.655	326.439	3.980	322.862	0.403
		DP500	322.534	322.649	331.893	9.456	323.065	0.628
S_{AB}	282.29	ST14F	281.808	281.728	282.138	0.25	281.920	0.032
		BH300	281.861	281.691	282.683	0.652	282.074	0.043
		DP500	281.836	281.657	283.557	1.542	282.230	0.215
S_{BC}	130.72	ST14F	130.702	130.702	131.609	0.907	130.800	0.098
		BH300	130.693	130.695	133.276	2.585	130.979	0.288
		DP500	130.680	130.687	137.350	6.677	131.198	0.525

		ST14F	188.841	188.938	189.005	0.261	188.776	0.032
S_{CD}	188.89	BH300	188.781	188.911	189.370	0.719	188.707	0.056
		DP500	188.780	188.889	190.317	1.646	188.928	0.257

Dev_{DA} defined in Equation (8) represents the difference between the length of a curve before springback and that after springback obtained using DA method while Dev_{sp-DA} represents the difference using SP-DA method.

$$\begin{cases} Dev_{DA} = \left|V_{DA} - \left[V_f + \left(V_f - V_s\right)\right]\right| \\ Dev_{sp-DA} = \left|V_{sp-DA} - \left[V_f + \left(V_f - V_s\right)\right]\right| \end{cases} \quad (8)$$

Fig. 16 shows the difference in DA method increase with the increase of springback. On the other hand, the effect of springback on the difference in SP-DA method is very small, which means SP-DA method is more accurate and reliable. SP-DA method converges in a stable way and is in particular effective when dealing with large springback.

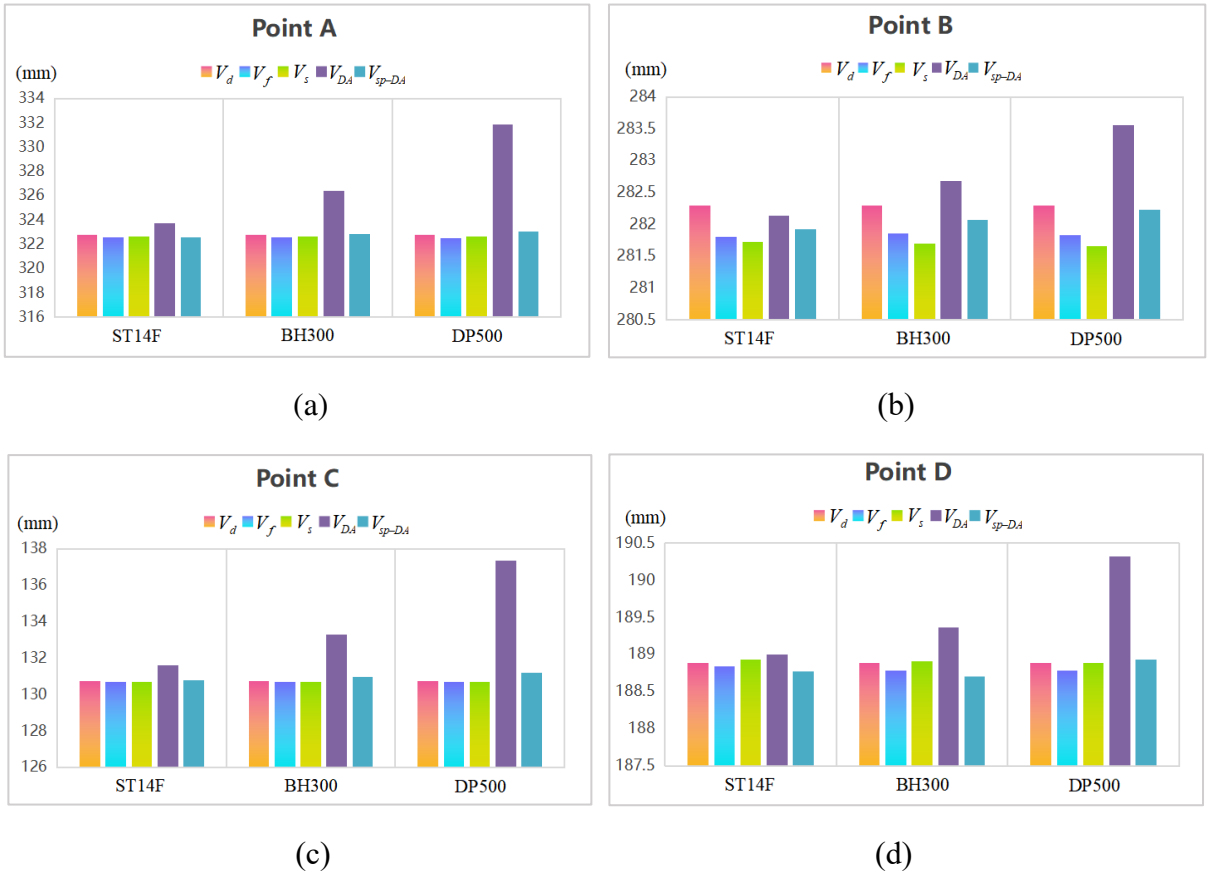

Figure 16 Comparison of the lengths of the four curves of three steels at locations A, B, C and D

3.2 Verification

It is necessary to verify the assumption made in the beginning, i.e. the moving path of a node during springback is always similar to the moving path of the node in springback compensation. The springback after stamping obtained in FEM analysis using the model of the

die modified based on SP-DA compensation and that based on the original design were compared. The results of steel BH300 shown in Fig. 17 are used for this verification.

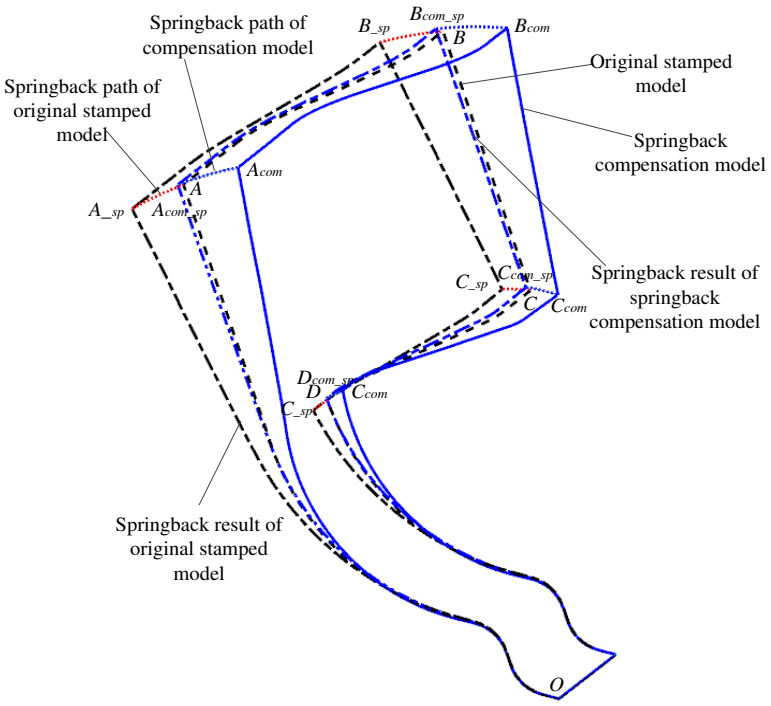

(a) Outlines of the simulation model

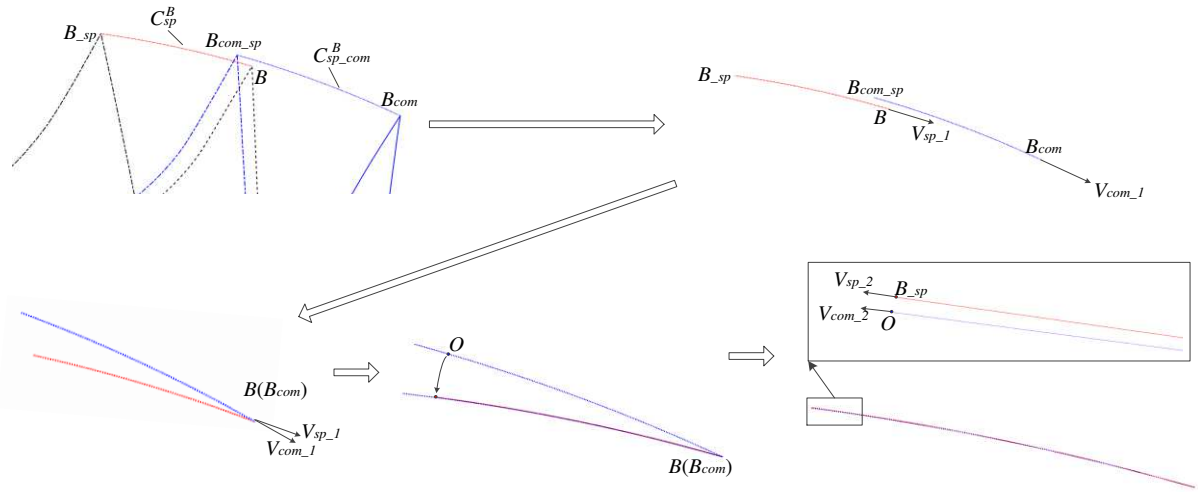

(b) Springback paths at location B

Figure 17. Comparison of the springback of steel BH300 after stamping obtained in FEM analysis using the model of the die modified based on SP-DA compensation and that based on the original design

Taking location B as an example, point B is in original design model and its position after springback is point B_{sp}. Point B_{com} is in springback compensation model and its position after

springback is point B_{com_sp}. The springback paths at location B are shown in Fig. 17 (b). C_{sp}^{B} is the springback path curve obtained in the original design model and V_{sp_1} is the tangent vector at point B. $C_{sp\_com}^{B}$ is the springback path curve obtained in the springback compensation model and V_{com_1} is the tangent vector at point B_{com_sp}. (1) To move C_{sp}^{B} and let point B coincide with point B_{com}; (2) To rotate $C_{sp\_com}^{B}$ about point B_{com} till V_{com_1} coincides with V_{sp_1}; (3) The length of $C_{sp\_com}^{B}$ is 35.895mm while that of C_{sp}^{B} is 32.315mm. $C_{sp\_com}^{B}$ is cut at point O from which to point B_{com} the length is equal that of C_{sp}^{B}; (4) V_{sp_2} is the tangent vector at point $B_{\_sp}$ on C_{sp}^{B}, and V_{com_2} is the tangent vector at point O of $C_{sp\_com}^{B}$. The angle θ between V_{sp_2} and V_{com_2}, and the distance Δ between point $B_{\_sp}$ and point O are measured.

The above was done at all four locations A, B, C and D and the results are shown in Table 8.

Table 8 Comparison between two springback paths obtained in the model modified using SP-DA method and that obtained in original design model

Location	$\boldsymbol{\theta}$ (degree)	Δ (mm)
A	0.820	0.096
B	0.558	0.079
C	0.524	0.080
D	1.104	0.081

It can be seen that both θ and Δ are very small, which means the two paths are highly similar, i.e. the assumption that the moving path of a node during springback is always similar to the moving path of the node in springback compensation can be verified.

4. Conclusion

This research proposed an enhanced hybrid springback compensation method named Springback Path – Displacement Adjustment (SP-DA) method. A model of stamping part owning sufficient geometry complexity was carefully designed. FEM simulation of a stamping process and analysis on springback were conducted. Low, medium and high strength steels adopted in automobile industry were considered. The results obtained using SP-DA method were compared with those using DA method. The results show the new SP-DA method is able to significantly improve the accuracy of springback compensation in sheeting metal forming of complex shaped product, on which the influence of high strength of the materials and high springback is minimized.

Declarations

Funding The National Natural Science Foundation of China (Grant No. 51975200) and the Natural Science Foundation of Hunan Province, China (Grant No. 2020JJ4189) are acknowledged for funding this research. Zhihui Gong was granted his visiting scholar fellowship by China Scholarship Council to conduct collaborative research as a visiting research fellow at University of Technology Sydney.

Competing interests The authors declare no competing interests.

Availability of data and material All data generated or analyzed during this study are included in this published article.

Ethics approval The article follows the guidelines of the Committee on Publication Ethics (COPE) and involves no studies on human or animal subjects.

Consent to participate All authors confirm that they are involved to this study

Consent for publication All authors have read and agreed to publish the manuscript.

References

[1] Spathopoulos S C, Stavroulakis G E. Springback Prediction in Sheet Metal Forming, Based on Finite Element Analysis and Artificial Neural Network Approach[J]. Applied Mechanics, 2020, 1(2): 97-110.

[2] Liang J C, Gao S, Teng F, et al. Flexible 3D stretch-bending technology for aluminum profile[J]. The International Journal of Advanced Manufacturing Technology, 2014, 71(9-12):1939-1947.

[3] Su C, Zhang K, Lou S, et al. Effects of variable blank holder forces and a controllable drawbead on the springback of shallow-drawn TA2M titanium alloy boxes[J]. The International Journal of Advanced Manufacturing Technology, 2017, 93(5): 1627-1635.

[4] Wei H, Zhou L, Heidarshenas B, et al. Investigation on the influence of springback on precision of symmetric-cone-like parts in sheet metal incremental forming process[J]. International Journal of Lightweight Materials and Manufacture, 2019, 2(2): 140-145.

[5] Troive L, Bałon P, Świątoniowski A, et al. Springback compensation for a vehicle's steel body panel[J]. International Journal of Computer Integrated Manufacturing, 2018, 31(2): 152-163.

[6] Farhadi A, Nayebi A. Springback analysis of thick-walled tubes under combined bending-torsion loading with consideration of nonlinear kinematic hardening[J]. Production Engineering, 2020, 14(2): 135-145.

[7] Marcondes P V P, dos Santos R A, Haus S A. The coining force influence on springback in TRIP800 steel V and L-bending processes[J]. Journal of the Brazilian Society of Mechanical Sciences and Engineering, 2016, 38(2): 455-463.

[8] Zhang S, Fu M, Wang Z, et al. Springback prediction model and its compensation method for the variable curvature metal tube bending forming[J]. The International Journal of Advanced Manufacturing Technology, 2021, 112(11): 3151-3165.

[9] Hajbarati H, Zajkani A. A novel analytical model to predict springback of DP780 steel based on modified Yoshida-Uemori two-surface hardening model[J]. International Journal of Material Forming, 2019, 12(3): 441-455.

[10] Liu X, Cao J, Huang S, et al. Experimental and numerical prediction and comprehensive compensation of springback in cold roll forming of UHSS[J]. The International Journal of Advanced Manufacturing Technology, 2020, 111(3): 657-671.

[11] Zhu H, Chang X, Jung D W. The generation of the forming path with the springback compensation in the CNC incremental forming[J]. International Journal of Material Forming, 2018, 11(4): 455-470.

[12] Wang H, Zhou J, Zhao T, et al. Springback compensation of automotive panel based on three-dimensional scanning and reverse engineering[J]. The International Journal of Advanced Manufacturing Technology, 2016, 85(5): 1187-1193.

[13] Dan J, Lancheng W. Direct generation of die surfaces from measured data points based on springback compensation[J]. The International Journal of Advanced Manufacturing Technology, 2006, 31(5): 574-579.
[14] Karafillis A P, Boyce M C. Tooling and binder design for sheet metal forming processes compensating springback error[J]. International Journal of Machine Tools and Manufacture, 1996, 36(4): 503-526.
[15] Wu L, Du C, Zhang L. Iterative FEM die surface design to compensate for springback in sheet metal stampings[C]//Proceedings of NUMIFORM. 1995, 95: 637-641.
[16] Wu L. Generate tooling mesh by FEM virtual forming model for springback compensation in die surface design of sheet metal stamping[J]. SAE transactions, 1996: 643-649.
[17] Anagnostou E L, Papazian J M. Optimized tooling design algorithm for sheet metal forming over reconfigurable compliant tooling[C]//AIP Conference Proceedings. American Institute of Physics, 2004, 712(1): 741-748.
[18] Gan W, Wagoner R H. Die design method for sheet springback[J]. International Journal of Mechanical Sciences, 2004, 46(7): 1097-1113.
[19]Weiher J, Rietman B, Kose K, et al. Controlling springback with compensation strategies[C]//AIP conference proceedings. American Institute of Physics, 2004, 712(1): 1011-1015.
[20] Yang X A, Ruan F. A die design method for springback compensation based on displacement adjustment[J]. International Journal of Mechanical Sciences, 2011, 53(5): 399-406.